Lovastatin regulates brain spontaneous low-frequency brain activity in Neurofibromatosis type 1

Camille Chabernaud, PhD[a], **Maarten Mennes, PhD**[a], **Peter G. Kardel, MA**[b], **William D. Gaillard, MD**[c], **M. Layne Kalbfleisch, PhD**[d], **John W. VanMeter, PhD**[e], **Roger J. Packer, MD**[b,c], **Michael P. Milham, MD, PhD**[f,g], **Francisco X. Castellanos, MD**[a,g], and **Maria T. Acosta, MD**[b,c]

[a]Phyllis Green and Randolph Cowen Institute for Pediatric Neuroscience at the New York University Langone Medical Center, 215 Lexington Avenue, New York, NY 10016, USA

[b]Jennifer and Daniel Gilbert Neurofibromatosis Institute, Children's National Medical Center, 111 Michigan Avenue NW, Washington D.C., 20010, USA

[c]The Center for Neuroscience and Behavioral Medicine, Children's National Medical Center, 111 Michigan Avenue NW, Washington D.C., 20010, USA

[d]KIDLAB, Krasnow Institute for Advanced Study and College of Education and Human Development, George Mason University, Mail Stop 2A1, Fairfax, VA 22030, USA

[e]Center for Functional and Molecular Imaging, Georgetown University Medical Center, 3900 Reservoir Rd. NW, Washington, D.C., 20057, USA

[f]Center for the Developing Brain, Child Mind Institute, 445 Park Avenue, New York, NY10022, USA

[g]Nathan Kline Institute for Psychiatric Research, 140 Old Orangeburg Road, Orangeburg, NY 10962, USA

Abstract

In the Neurofibromatosis type 1 (NF1) mouse model, lovastatin, used clinically for hypercholesterolemia, improves cognitive dysfunction. While such impairment has been studied in NF1, the neural substrates remain unclear. The aim of this imaging add-on to a phase-1 open-label trial was to examine the effect of lovastatin on Default Network (DN) resting state functional connectivity (RSFC). Seven children with NF1 (aged 11.9±2.2; 1 female) were treated with lovastatin once daily for 12 weeks. A 7-minute 3-Tesla echo-planar-imaging scan was collected one day before beginning treatment (off-drug) and the last day of treatment (on-drug) while

Corresponding author: Maria T. Acosta, MD, Jennifer and Daniel Gilbert Neurofibromatosis Institute, Children's National Medical Center, Washington D.C., USA, 111 Michigan Av. NW, Washington DC, 20010, Phone: 202-476-2120, Fax: 202-476-5265, macosta@childrensnational.org.

performing a Flanker task. After regressing-out task-associated variance, we used the residual time series as "continuous resting-state data" for RSFC analyses using 11 DN regions of interest. For qualitative comparisons, we included a group of 19 typically developing children (TDC) collected elsewhere. In the on-drug condition, lovastatin increased long-range positive RSFC within DN core regions (i.e., anterior medial prefrontal cortex and posterior cingulate cortex, PCC). In addition, lovastatin produced less diffuse local RSFC in the dorsomedial prefrontal cortex and PCC. The pattern of RSFC observed in the NF1 participants when on-drug closely resembled the RSFC patterns exhibited by the TDC. Lovastatin administration in this open trial regulated anterior-posterior long-range and local RSFC within the DN. These preliminary results are consistent with a role for lovastatin in normalization of developmental processes and with apparent benefits in a mouse NF1 model.

Keywords

Introduction

Neurofibromatosis type 1 (NF1) is one of the most frequent autosomal genetic disorders, affecting one in 3000 newborns [19]. Besides the typical diagnostic symptoms associated with neurofibromatosis, between 30 and 65% of children with NF1 exhibit learning disabilities and cognitive deficits such as visuospatial or executive dysfunction [20]. Due to their high incidence, neurocognitive impairments are considered the most functionally disruptive chronic disabilities in children with NF1 [1].

The NF1 gene encodes neurofibromin, a protein underlying several functions including inhibition of p21Ras GTPase-activating protein activity [5]. The increase in p21Ras activity, caused by mutations of the NF1 gene, has been related to the learning deficits observed in NF1 mice and in humans, leading to the hypothesis that inhibition of Ras activity may reverse these cognitive deficits [10, 22]. Because posttranslational farnelysation is required for p21Ras function, farnelysation has been suggested as a pharmacotherapy target for NF1 cognitive deficits. Previous studies demonstrated that lovastatin, a 3-hydroxy-3-methylglutaryl coenzyme A reductase inhibitor, successfully inhibits p21Ras isoprenylation and activity [27]. Examining the effects of lovastatin on cognitive deficits, Li et al. reported that lovastatin effectively decreased p21Ras activity and reversed attention and learning deficits observed in *Nf1*+/− mice [24]. While the results of statin therapy in mice models are encouraging, simvastatin used in humans did not yield similar results [23]. However, as part of a Phase 1 open-label safety trial, significant cognitive improvements were found comparing pre- and post-lovastatin treatment, suggesting that lovastatin might be effective for treating cognitive deficits in children with NF1 [2].

Cognitive dysfunction in children with NF1 has been extensively examined at the behavioral level [20]. However, the specific brain correlates of such deficits in NF1 are poorly understood. Previous functional magnetic resonance imaging (fMRI) studies indicated that children with NF1 recruit different brain areas during various cognitive tasks relative to typically developing children (TDC) [7, 8]. For example, Billingsley et al. reported greater activation of posterior regions (i.e., temporal, parietal and occipital cortex) relative to anterior regions (i.e., inferior and lateral orbital frontal cortex) during visuo-spatial performance in children with NF1 relative to controls [8]. Overall, findings from fMRI studies in children with NF1 suggest that functional interactions between neural networks, rather than dysfunction in a specific brain area, might underlie the cognitive deficits frequently observed in this disease.

Resting state functional connectivity (RSFC) approaches can successfully delineate functional brain networks without external stimulation [9]. A myriad of functional networks can be revealed through patterns of synchrony in spontaneous, low-frequency brain activity, that are remarkably similar to functional networks observed in task-based fMRI approaches [29]. Here, we examined the effects of 12-week lovastatin treatment on the RSFC of the default network (DN), one of the main intrinsic functional brain networks, on seven children with NF1 who were part of a Phase 1 open label trial [2]. Based on previous findings of neuronal dysfunction in children with NF1, we expected that lovastatin would significantly improve and normalize DN organization.

Methods

Participants

Seven children with NF1 (age 11.9±2.2 yrs; range: 10–15; 1 female) participated in this study. The diagnosis was established according to National Institutes of Health international criteria (Neurofibromatosis Conference Statement, 1987). Inclusion criteria required full-scale IQ above 80 and absence of any other chronic medical condition or symptomatic complication. The study was approved by the institutional review boards of Georgetown University, Children's National Medical Center, New York University (NYU) and NYU School of Medicine. Prior to participation, written assent and consent were obtained from children and their parents/legal guardian respectively, in accordance with the Declaration of Helsinki.

In the absence of imaging data from TDC scanned at Georgetown University, we included data from 19 TDC scanned at the NYU Center for Brain Imaging for qualitative comparisons (age 13.2±2.5 yrs; range: 9–16; 3 females). The TDC and patients were group-matched on age (t=−1.17, p=0.27), estimated IQ (95±10 and 88±6 respectively, t=−2.07, p=0.054) and sex ($\chi^2_{(1)}$=0.01, p=.92).

Lovastatin Protocol

Each patient was treated with lovastatin once daily for 12 weeks after breakfast (weeks 0–4, 20 mg/d; weeks 5–8, 30 mg/d; and weeks 9–12, 40 mg/d). Pre-treatment laboratory tests were performed on day one of the study, including complete blood count, blood urea nitrogen, creatinine, glucose, alanine amino transferase, aspartate amino transferase, bilirubin, creatine phosphokinase, lipid profile (total cholesterol, HDL, vLDL, LDL, triglycerides), urinalysis, and a urine pregnancy test (females only). A monthly clinic visit and phone calls at weeks 1, 2, and 3 were completed to support and document compliance and side effects during the escalation dose period. As described elsewhere, participants underwent cognitive testing prior to treatment initiation (baseline) and post 12-week open treatment [2]. Cognitive measures included the Test of Everyday Attention for Children (TEA-Ch), the California Verbal Learning Test for Children (CVLT) and the Wide Range Assessment of Memory and Learning, Second Edition (WRAML-2) [2].

Imaging Protocol

Imaging data from patients were acquired using a Siemens Magnetom Trio 3-Tesla scanner at the Center for Functional and Molecular Imaging at Georgetown University. For each participant, a 7-minute echo-planar imaging scan was collected one day prior to beginning treatment (off-drug) and on the last day of the 3-month trial (on-drug) (TR=3000 ms; TE=30 ms; flip angle=90°, 39 slices, matrix=64×64; FOV=192 mm; acquisition voxel size= 3×3×3 mm). All scans were collected in the early afternoon (~6 hours after daily dose of drug consumed). The children were scanned while performing a version of the flanker task based on the Naglieri Nonverbal Ability Test (NNAT) licensed to MLK. Each child performed two

runs, each of which contained 4 blocks, 2 with congruent flankers (e.g., <<<<<) and 2 with incongruent flankers (e.g., >><>>) presented in ABBA order. Stimulus duration was 1200ms with a 1200ms inter-trial interval. The resting epoch between blocks was 4800ms long. For the analyses presented here, we regressed out the task-induced BOLD variance from the event-related data, producing residuals that are considered comparable to "continuous resting-state" data [15]. Subsequent analyses were then performed using these residuals, which we considered a "pseudo-resting state" signal, parsed out/aggregated from motion and physiological noise. For registration and analysis purposes, a T1-weighted anatomical image was also acquired using a magnetization prepared gradient echo sequence (TR/TE 9.7/4ms, 256×256 FOV, 160mm slab thickness, 256×256×160 matrix (effective resolution 1mm^3), 1 excitation, 12° flip angle). Imaging data from TDC were acquired using a Siemens Allegra 3-Tesla scanner at the NYU Center for Brain Imaging. For each TDC participant, a 6-min resting scan comprising 180 contiguous whole-brain functional volumes was acquired using a multi-echo echo-planar imaging sequence (TR=2000ms; flip angle=90°; 33 slices; voxel size=3×3×4mm; effective TE=30ms, FOV=240×192mm). A T1-weighted anatomical image was also acquired using a magnetization prepared gradient echo sequence (TR=2530ms; TE=3.25ms; TI=1100ms; flip angle=7°; 128 slices; FOV=256mm; acquisition voxel size=1.3×1×1.3mm).

Image preprocessing

We used a combination of AFNI (http://afni.nimh.nih.gov/afni/) and the FMRIB software library tool (FSL, www.fmrib.ox.ac.uk) to preprocess the EPI scans. Details regarding the preprocessing steps are provided in Supplementary S1.

Nuisance and task-induced BOLD signal regression

To control for motion and physiological nuisance signals (e.g., cardiac and respiratory fluctuations), we regressed the preprocessed data on nine nuisance covariates, removing variance associated with non-neuronal signals derived from white matter, cerebrospinal fluid, the global signal and six motion parameters [21]. Subsequently we regressed the resultant 4-D residual time series on a covariate modeling all trials presented during the flanker task [15]. The residuals resulting from this analysis are considered a valid "pseudo-resting state" signal [15].

Selection of regions of interest (ROIs)

We used 11 DN ROIs ("seeds") as defined previously [4]. The seeds comprised: Anterior Medial Prefrontal Cortex (aMPFC) and Posterior Cingulate Cortex (PCC) representing the midline core subsystem; Temporo-Parietal Junction (TPJ), Lateral Temporal Cortex (LTC), Temporal Pole (TempP), Dorsal Medial Prefrontal Cortex (dMPFC) and Ventral Medial Prefrontal Cortex (vMPFC), constituting the dMPFC subsystem; Posterior Inferior Parietal Lobule (pIPL), Retrosplenial Cortex (Rsp), Parahippocampal Cortex (PHC) and Hippocampal Formation (HF), constituting the Medial Temporal Lobe (MTL) subsystem. For each region, we created a spherical seed ROI (4mm radius), centered on published coordinates [4].

Participant-level RSFC analysis

For each participant, the representative time series for each seed ROI was extracted from their 4D residualized standard-space pseudo-resting state volume by averaging the time series across all voxels within the ROI. We then calculated the correlation between each seed ROI time series and that of every other voxel in the brain. The resultant participant-level correlation maps were Fisher-z transformed to improve normal distribution and transformed into MNI152 2mm standard space for group-level analyses.

Group-level RSFC analysis

For each seed, group-level analyses were performed to compare off- and on-drug conditions using a within-participant repeated measures mixed-effects ordinary least-squares model as implemented in FSL. This group-level analysis produced thresholded Z-score maps of positive and negative connectivity for each DN ROI and for each condition. Direct condition comparisons produced thresholded Z-score maps for each ROI of those voxels that showed significant lovastatin-related changes in functional connectivity with each ROI. Recent reports have pointed out the influence of small head movements on RSFC timecourses and have suggested that standard regression analyses may not be sufficient to fully account for head motion [26, 31]. To account for head motion micro-movements in our analyses, we calculated the mean of frame displacement for each subject and used it as a covariate. For all analyses, corrections for multiple comparisons were performed at the cluster level using Gaussian random field theory (min $Z > 2.3$; cluster significance: $p < 0.0045$, corrected, to account for the 11 seeds analyzed [0.05/11 = 0.0045]).

Results

Regression analyses revealed that functional connectivity within the DN differed significantly between off- and on-drug conditions (Table 1). In particular, two main changes were observed between conditions: increased long-range positive connectivity and decreased local functional connectivity.

Lovastatin increases long-range functional connectivity within DN regions

When comparing the off- and on-drug conditions, we observed enhanced positive functional connectivity between core DN regions (i.e., aMPFC and PCC). In particular, during the off-drug condition, typical long-range RSFC between the PCC and aMPFC was absent (Figure 1). In contrast, during the on-drug scan, a significant long-range positive relationship emerged between these two regions (Figure 1). Importantly, the on-drug RSFC of children with NF1 closely resembled the connectivity pattern exhibited by the TDC. The increase of RSFC along the anterior-posterior axis was also highlighted for connectivity of the dMPFC seed with the PCC (see Supplementary S2) and between the Rsp seed and the medial prefrontal cortex (see Supplementary S3).

Lovastatin regulates focal functional connectivity within DN regions

During the off-drug condition, local functional connectivity (i.e., RSFC near the seed region) was significantly more diffuse than during the on-drug condition. Specifically, for the PCC seed, we observed significantly more diffuse and aberrant RSFC in the temporal cortex during the off-drug relative to the on-drug condition (Figure 1). A comparable pattern was observed in the TDC. We found similar results for the dMPFC seed, with significantly greater positive RSFC in the rostral section of the supragenual anterior cingulate cortex (ACC) during the off-drug condition (See Supplementary S2), and for the Rsp seed, which exhibited significantly greater aberrant short-range positive connectivity with the lingual gyrus (See Supplementary S3). This connectivity was not present during the on-drug condition, or in the TDC. Finally, similar results were observed for connectivity between the TempP seed and the Supramarginal gyrus (See Supplementary S4), with decreased connectivity observed during the on-drug condition.

Lovastatin also regulated negative RSFC relationships within the DN. Specifically, we observed a significantly greater negative relationship between the vMPFC and the superior parietal lobule during off-drug condition, a pattern which was not present either in TDC or in the patients on-drug (See Supplementary S5).

Although not the focus of this preliminary study, we note significant post-treatment improvements only on WRAML-2 Story Memory ($t_{(7)}$=2.81, p=.03), WRAML-2 Design Memory ($t_{(7)}$=4.42, p=.005), and WRAML-2 Symbolic Working Memory ($t_{(7)}$=2.76, p=.03). These did not correlate significantly with change in RSFC beyond chance expectations.

Discussion

Using R-fMRI to investigate the effects of lovastatin on default network (DN) functional connectivity, we observed several significant abnormalities in the patterns of synchrony in spontaneous low frequency fluctuations in children affected with NF1 at baseline. Following 12-week open treatment with lovastatin [2], we detected significant changes in within-DN long-range RSFC consistent with normalization. In the on-drug condition, we also observed more focal local (short-range) RSFC. Taken together, these observations mirror the patterns of RSFC reported in cross-sectional studies of typical development, that short-range functional connectivity decreases and long-range functional connectivity increases across development [14, 21]. Such conclusions have also been supported by reports of a shift from diffuse to focal activation patterns in task-based functional imaging studies [13].

The DN is typically activated when participants are not engaged in attentionally demanding tasks and is deactivated during stimulus-driven activity [16, 30]. These observations led to the idea that the DN underlies spontaneous cognitive processes including making predictions about the future or affective decision-making [3]. However, the PCC and the aMPFC have been reported to be significantly positively correlated during rest as well as during working memory processing [18]. In that study, the strength of the PCC-aMPFC correlation was positively associated with better working memory performance leading to the suggestion that the core regions of the DN may work together to facilitate cognitive processing. Accordingly, we speculate that alteration of DN functional connectivity may underlie some of the cognitive deficits observed in children with NF1 and that regulating its functional connectivity may contribute to improved cognitive performance. Studies with larger sample sizes will be needed to assess this hypothesis.

Lovastatin therapy significantly increased long-range RSFC in children with NF1, qualitatively approaching RSFC patterns observed in TDC. These changes paralleled but did not correlate significantly with significant improvements in memory performance. The diffusion tensor imaging apparent diffusion coefficient (ADC) is interpreted as an index of axon packing, internal axon structure and myelination [6]. Significantly higher ADC, particularly in frontal and parieto-occipital white matter, has been reported in children with NF1 relative to controls [32]. Such microstructural abnormalities may underlie the DN RSFC alterations we observed, as suggested by the finding of a close relationship between tractography linking the aMPFC and PCC and their functional connectivity [17]. In NF1, deficient neurofibromin expression, the product of the NF1 gene, affects astrocyte growth and differentiation and impairs somatosensory cortical development [11, 25]. Together, these findings suggest that alteration of neurofibromin expression likely impacts brain development, affecting both structural and functional connectivity.

Our results should be examined in light of limitations. Given the small sample size, which reflected the nature of Phase I studies, our results are preliminary. The most important limitation is that order of scan acquisition was not counter-balanced, as all children were naïve to lovastatin at baseline. While we cannot exclude the possibility that our findings of DN RSFC modulation reflect maturation over the three-month period or habituation to the scanner environment, this possibility is not supported by the moderate to high test-retest reliability of RSFC in adults, nor by the cross-sectional data on RSFC maturation from 7 to 30 years of age [12, 28]. Future studies should exclude the potential effect of order and re-

scanning by counter-balancing on- and off-drug scans. Although event-related data residuals are qualitatively and quantitatively very similar to continuous resting-state data, some differences should be noted. Specifically, task engagement might reduce spontaneous fluctuations in brain activity, leading to stronger correlations in some regions during continuous resting-state data [15]. In conclusion, although replication in larger samples with counter-balancing of medication administration is needed, our results suggest the intriguing possibility that lovastatin enhances maturation of DN brain functional connectivity in children with NF1 and that such changes may underlie improvements in cognitive function.

Conclusions

This preliminary report of brain biomarkers in the context of a phase-1 open-label trial suggests resting-state functional MRI will be a useful and powerful approach for assessing the pharmacological responses of potential treatments such as lovastatin, even in limited samples.

Highlights

- We examined brain functional connectivity changes associated with lovastatin treatment

- Lovastatin regulated functional connectivity in Neurofibromatosis type 1

- Lovastatin produced increased long-range positive resting-state functional connectivity

- Lovastatin produced less diffuse local resting-state functional connectivity

Supplementary Material

Refer to Web version on PubMed Central for supplementary material.

Acknowledgments

References

1. Acosta MT, Gioia GA, Silva AJ. Neurofibromatosis type 1: new insights into neurocognitive issues. Curr Neurol Neurosci Rep. 2006; 6:136–143. [PubMed: 16522267]

2. Acosta MT, Kardel PG, Walsh KS, Rosenbaum KN, Gioia GA, Packer RJ. Lovastatin as treatment for neurocognitive deficits in neurofibromatosis type 1: phase I study. Pediatr. Neurol. 2011; 45:241–245. [PubMed: 21907886]

3. Andrews-Hanna JR, Reidler JS, Huang C, Buckner RL. Evidence for the default network's role in spontaneous cognition. J. Neurophysiol. 2010b; 104:322–335. [PubMed: 20463201]

4. Andrews-Hanna JR, Reidler JS, Sepulcre J, Poulin R, Buckner RL. Functional-Anatomic Fractionation of the Brain's Default Network. Neuron. 2010a; 65:550–562. [PubMed: 20188659]

5. Ballester R, Marchuk D, Boguski M, Saulino A, Letcher R, Wigler M, Collins F. The NF1 locus encodes a protein functionally related to mammalian GAP and yeast IRA proteins. Cell. 1990; 63:851–859. [PubMed: 2121371]

6. Basser PJ, Jones DK. Diffusion-tensor MRI: theory, experimental design and data analysis - a technical review. NMR Biomed. 2002; 15:456–467. [PubMed: 12489095]

7. Billingsley RL, Jackson EF, Slopis JM, Swank PR, Mahankali S, Moore BD 3rd. Functional magnetic resonance imaging of phonologic processing in neurofibromatosis 1. J. Child Neurol. 2003; 18:731–740. [PubMed: 14696899]

8. Billingsley RL, Jackson EF, Slopis JM, Swank PR, Mahankali S, Moore BD III. Functional MRI of visual-spatial processing in neurofibromatosis, type 1. Neuropsychologia. 2004; 42:395–404. [PubMed: 14670578]

9. Cole DM, Smith SM, Beckmann CF. Advances and pitfalls in the analysis and interpretation of resting-state FMRI data. Front Syst Neurosci. 2010; 4:8. [PubMed: 20407579]

10. Costa RM, Federov NB, Kogan JH, Murphy GG, Stern J, Ohno M, Kucherlapati R, Jacks T, Silva AJ. Mechanism for the learning deficits in a mouse model of neurofibromatosis type 1. Nature. 2002; 415:526–530. [PubMed: 11793011]

11. Dasgupta B, Gutmann DH. Neurofibromin regulates neural stem cell proliferation, survival, and astroglial differentiation in vitro and in vivo. J. Neurosci. 2005; 25:5584–5594. [PubMed: 15944386]

12. Dosenbach NU, Nardos B, Cohen AL, Fair DA, Power JD, Church JA, Nelson SM, Wig GS, Vogel AC, Lessov-Schlaggar CN, Barnes KA, Dubis JW, Feczko E, Coalson RS, Pruett JR Jr, Barch DM, Petersen SE, Schlaggar BL. Prediction of individual brain maturity using fMRI. Science. 2010; 329:1358–1361. [PubMed: 20829489]

13. Durston S, Davidson MC, Tottenham N, Galvan A, Spicer J, Fossella JA, Casey BJ. A shift from diffuse to focal cortical activity with development. Dev Sci. 2006; 9:1–8. [PubMed: 16445387]

14. Fair DA, Cohen AL, Dosenbach NU, Church JA, Miezin FM, Barch DM, Raichle ME, Petersen SE, Schlaggar BL. The maturing architecture of the brain's default network. Proc. Natl. Acad. Sci. U. S. A. 2008; 105:4028–4032. [PubMed: 18322013]

15. Fair DA, Schlaggar BL, Cohen AL, Miezin FM, Dosenbach NU, Wenger KK, Fox MD, Snyder AZ, Raichle ME, Petersen SE. A method for using blocked and event-related fMRI data to study "resting state" functional connectivity. Neuroimage. 2007; 35:396–405. [PubMed: 17239622]

16. Fransson P. How default is the default mode of brain function? Further evidence from intrinsic BOLD signal fluctuations. Neuropsychologia. 2006; 44:2836–2845. [PubMed: 16879844]

17. Greicius MD, Supekar K, Menon V, Dougherty RF. Resting-state functional connectivity reflects structural connectivity in the default mode network. Cereb. Cortex. 2009; 19:72–78. [PubMed: 18403396]

18. Hampson M, Driesen NR, Skudlarski P, Gore JC, Constable RT. Brain connectivity related to working memory performance. J. Neurosci. 2006; 26:13338–13343. [PubMed: 17182784]

19. Huson SM, Compston DA, Clark P, Harper PS. A genetic study of von Recklinghausen neurofibromatosis in south east Wales. I. Prevalence, fitness, mutation rate, and effect of parental transmission on severity. J. Med. Genet. 1989; 26:704–711. [PubMed: 2511318]

20. Hyman SL, Shores A, North KN. The nature and frequency of cognitive deficits in children with neurofibromatosis type 1. Neurology. 2005; 65:1037–1044. [PubMed: 16217056]

21. Kelly AM, Di Martino A, Uddin LQ, Shehzad Z, Gee DG, Reiss PT, Margulies DS, Castellanos FX, Milham MP. Development of anterior cingulate functional connectivity from late childhood to early adulthood. Cereb. Cortex. 2009; 19:640–657. [PubMed: 18653667]

22. Klose A, Ahmadian MR, Schuelke M, Scheffzek K, Hoffmeyer S, Gewies A, Schmitz F, Kaufmann D, Peters H, Wittinghofer A, Nurnberg P. Selective disactivation of neurofibromin GAP activity in neurofibromatosis type 1. Hum. Mol. Genet. 1998; 7:1261–1268. [PubMed: 9668168]

23. Krab LC, de Goede-Bolder A, Aarsen FK, Pluijm SM, Bouman MJ, van der Geest JN, Lequin M, Catsman CE, Arts WF, Kushner SA, Silva AJ, de Zeeuw CI, Moll HA, Elgersma Y. Effect of simvastatin on cognitive functioning in children with neurofibromatosis type 1: a randomized controlled trial. JAMA. 2008; 300:287–294. [PubMed: 18632543]

24. Li W, Cui Y, Kushner SA, Brown RA, Jentsch JD, Frankland PW, Cannon TD, Silva AJ. The HMG-CoA reductase inhibitor lovastatin reverses the learning and attention deficits in a mouse model of neurofibromatosis type 1. Curr. Biol. 2005; 15:1961–1967. [PubMed: 16271875]

25. Lush ME, Li Y, Kwon CH, Chen J, Parada LF. Neurofibromin is required for barrel formation in the mouse somatosensory cortex. J. Neurosci. 2008; 28:1580–1587. [PubMed: 18272679]

26. Power JD, Barnes KA, Snyder AZ, Schlaggar BL, Petersen SE. Spurious but systematic correlations in functional connectivity MRI networks arise from subject motion. Neuroimage. 2011

27. Sebti SM, Tkalcevic GT, Jani JP. Lovastatin, a cholesterol biosynthesis inhibitor, inhibits the growth of human H-ras oncogene transformed cells in nude mice. Cancer Commun. 1991; 3:141–147. [PubMed: 2043425]

28. Shehzad Z, Kelly AM, Reiss PT, Gee DG, Gotimer K, Uddin LQ, Lee SH, Margulies DS, Roy AK, Biswal BB, Petkova E, Castellanos FX, Milham MP. The resting brain: unconstrained yet reliable. Cereb. Cortex. 2009; 19:2209–2229. [PubMed: 19221144]

29. Smith SM, Fox PT, Miller KL, Glahn DC, Fox PM, Mackay CE, Filippini N, Watkins KE, Toro R, Laird AR, Beckmann CF. Correspondence of the brain's functional architecture during activation and rest. Proc. Natl. Acad. Sci. U. S. A. 2009; 106:13040–13045. [PubMed: 19620724]

30. Tomasi D, Ernst T, Caparelli EC, Chang L. Common deactivation patterns during working memory and visual attention tasks: an intra-subject fMRI study at 4 Tesla. Hum. Brain Mapp. 2006; 27:694–705. [PubMed: 16404736]

31. Van Dijk KRA, Sabuncu MR, Buckner RL. The influence of head motion on intrinsic functional connectivity MRI. Neuroimage. 2012; 59:431–438. [PubMed: 21810475]

32. van Engelen SJ, Krab LC, Moll HA, de Goede-Bolder A, Pluijm SM, Catsman-Berrevoets CE, Elgersma Y, Lequin MH. Quantitative differentiation between healthy and disordered brain matter in patients with neurofibromatosis type I using diffusion tensor imaging, AJNR. Am. J. Neuroradiol. 2008; 29:816–822. [PubMed: 18339726]
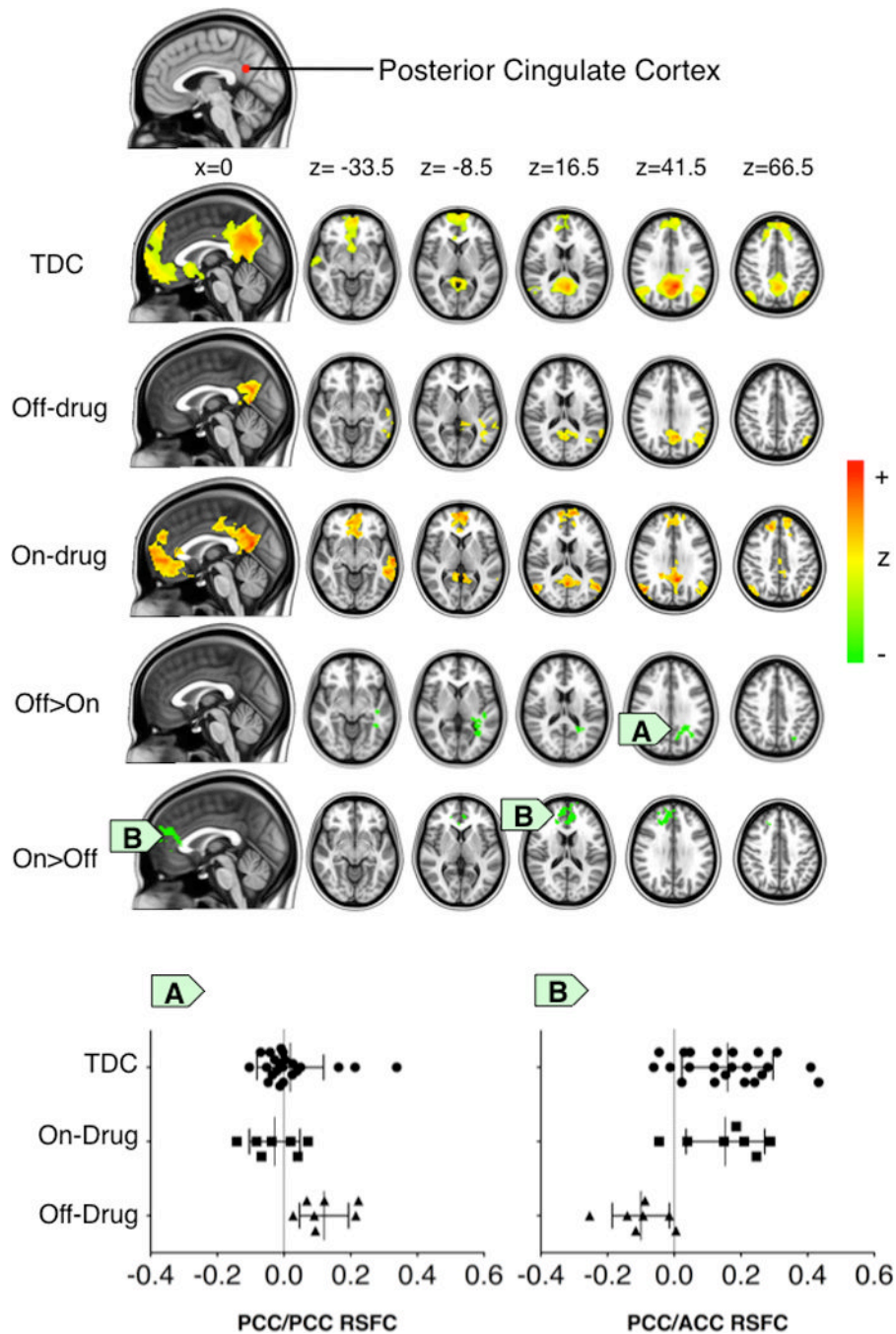
Figure 1. Positive functional connectivity between the posterior cingulate cortex (PCC) seed and every other voxel in the brain

The figure displays the thresholded Z-score maps of positive resting state functional connectivity (RSFC) with the PCC seed for each group and condition (typically developing children (TDC and patients with NF1 while off- or on-drug conditions). The Off>On and the On>Off maps respectively illustrate: A) the significant decrease in positive RSFC around the PCC and B) the significant increase of the positive RSFC between the PCC and the anterior cingulate cortex (ACC) in the NF1 on-drug condition relative to the NF1 off-drug condition. Accordingly, for each group and condition, the scatter plots illustrate functional connectivity (mean correlation coefficients) between the PCC region-of-interest and the

clusters exhibiting the significant Off>On and On>Off drug effect. Cluster-level Gaussian random field theory was employed for multiple comparison correction (Z>2.3; p<0.0045, corrected).

Table 1

Clusters of connectivity that showed a significant difference between baseline and after 12-weeks Lovastatin therapy, for each of the Default Network seeds

	Clusters size	Center of mass			p
		x	y	z	
dMPFC					
Off>On	1658	50	39	39	<0.0001
On>Off	1601	37	36	44	<0.0001
PCC					
Off>On	776	57	37	50	0.004
On>Off	1495	37	84	40	<0.0001
Rsp					
Off>On	1570	24	36	27	<0.0001
TempP					
Off>On	675	12	40	48	0.002
vMPFC					
Off>On	822	72	45	60	0.0003

dMPFC: dorsal medial prefrontal cortex, PCC: posterior cingulate cortex, Rsp: retrosplenial cortex, TempP: temporal pole, vMPFC: ventral medial prefrontal cortex